Influence of Draft Curtains on Sprinkler Activation – Comparison of Three Different Models

BJARNE PAULSEN HUSTED*

Danish Institute of Fire and Security Technology
Jernholmen 12, 2650 Hvidovre, Denmark

GÖRAN HOLMSTEDT

Department of Fire Safety Engineering, Lund University
Box 118, S-221 00 Lund, Sweden

ABSTRACT: This article investigates the importance of using draft curtains to obtain faster sprinkler activation with three different models-two computational fluid dynamics (CFD) models (CFX 4.4 and fire dynamics simulator (FDS) 4.07) and a zone model (Argos) containing a ceiling-jet formula - for an actual scenario in an entertainment center in Denmark. It is found that a draft curtain has some effect on sprinkler activation, reducing activation time from 8% to 15%, depending on the model implemented. The positions of the sprinklers with in the vertical computational grid of the CFD simulations have a greater influence on the activation of the sprinkler, where FDS is more sensitive than CFX. It is confirmed that heat transfer from the ceiling jet to the ceiling has little influence on the results. The zone model with a ceiling-jet formula gives 10–20% slower sprinkler activation than the CFD results when the sprinkler is close to the ceiling, but is still considered very useful in view of the faster calculation time.

KEY WORDS: ceiling jet, draft curtain, CFX, FDS, Argos, sprinkler activation, fire safety engineering.

INTRODUCTION

CALCULATION OF THE response of sprinklers plays an important role in performance based fire safety engineering. This is due to the fact that early activation of sprinklers means there is a better chance for sprinklers to

*Author to whom correspondence should be addressed. E-mail: bph@dbi-net.dk

1042-3915/08/01 0029–26 $10.00/0 DOI: 10.1177/1042391507080813

SAGE Publications, Los Angeles, London, New Delhi and Singapore

control the fire. In Denmark, there has been increased focus on the use of draft curtains so as to reduce the activation time of sprinklers. The fire authority has in some cases demanded draft curtains, a requirement opposed by the building owner because of extra cost and also opposed by the architect, as it would interfere with the architectural integrity and sense of open space in the building.

Traditionally, Alpert's ceiling jet formula [1] has been used in conjunction with zone models to calculate the response of sprinklers. This is the case for the zone models BRANZFIRE [2] and Argos [3], whereas the probably most well known zone model CFAST [4] uses the approach by Cooper [5]. Beyler [6] studied several different empirical ceiling jet formulas, including Alpert's formula. These formulas assume that there are no walls or other obstructions, which could lead to the formation of a hot layer. Beyler concluded that ignoring walls represents a conservative strategy. He also points out that Cooper [7], in an earlier work, showed that the heat loss to the ceiling is remarkably insensitive to the ceiling material. Several tests in this area have been done in the past. Nam [8] studied the actuation of sprinklers in rooms with high ceilings. He concluded that tests using pan fires, with their constant heat release rate (HRR), could lead to incorrect conclusions about the activation of sprinklers when compared to a fire with an increasing HRR. Motevalli [9] found that a combination of empirical velocity profiles and continuity and energy equations taking into account turbulence provided a good model for estimating ceiling jet flow. He concluded that the transient ceiling jet could be predicted using numerical tools with reasonable accuracy.

Heskestad and Hamada [10] made measurements of the temperature in the ceiling jet resulting from a strong fire plume but they only measured the temperature at one vertical position, 0.02 H below the ceiling. No velocities were measured. Hara and Kato [11], using the $k-\varepsilon$ model, did extensive computational fluid dynamics (CFD) calculations on the experimental results of Heskestad and Hamada, but could only compare them with the temperatures in the ceiling jet, as the velocity was not measured. Other experiments by Dembsey et al. [12] measured the ceiling jet temperature at 0.05 H below the ceiling. Murakami et al. [13] did steady-state measurements with laser Doppler anemometry (LDA) in a fire room but the heat source used was a heated plate. The preceding indicates there is a lack of good experimental data for a transient jet that is based on modern measurement techniques with good resolution in the vertical direction. Modern measurement techniques would include thin thermo-elements, particle image velocimetry, and LDA. Davis et al. [14] carried out CFD simulations to determine detector placement rules, but a rather coarse grid was used to resolve the ceiling jet.

Increasingly, CFD is used to predict smoke spread, as these models handle complex geometries better. Hence, sprinkler activation can be calculated directly from the CFD results, which contain information about velocities and temperatures in the ceiling jet, thereby avoiding the use of empirical formulas, which are only valid under certain conditions (e.g., flat ceilings and infinite distance to walls). However, the geometrical resolution required puts high demands on the grid density. General CFD programs like CFX [15] require users to write their own software for calculation of sprinkler response from the simulated temperature and flow field, whereas specialized CFD programs for fires, like fire dynamics simulator (FDS) [16], have built-in models for predicting the activation of sprinklers. McGrattan et al. [17] found that sprinkler activation for the first ring of sprinklers was predicted within 15% of the experimental results when using an earlier version of FDS, so sprinkler activation can be calculated with reasonable accuracy.

This article focuses on the influence of using a draft curtain to enhance sprinkler activation. Some further general conclusions will be drawn on modeling of the activation of heat detectors in two common CFD-programs used for fire modeling, the RANS model in CFX 4.4 [15] and the large eddy simulation (LES) model in FDS 4.07 [16], compared with Alpert's formula. Table 1 gives an overview of the simulations carried out.

GEOMETRY AND FIRE SCENARIO

The actual geometry is an entertainment center in Denmark, with a number of gaming machines in the basement of the building. From the basement, a stairway leads to the level above. Just near the foot of the stairway, the ceiling is raised to a height of 2.9 m, as shown in Figure 1. The dimension of the raised area is 3 m × 6 m. The ceiling height in the rest of the basement is 2.5 m. The main focus is the area around the raised ceiling, where smoke can escape to the floor above. A draft curtain at the edge of the raised ceiling can lead to the formation of a hot smoke layer and possibly earlier action of sprinklers situated under the raised ceiling. The draft curtain has a depth of 0.4 m. The geometry is symmetrical and the symmetry line is indicated in Figure 1.

The fire was modeled with the t^2-HRR given in Equation (1), which is similar to a medium fire according to the NFPA 204 [18]. The maximum HRR is 5 MW, but all sprinklers are activated before the maximum HRR is reached. The radiation fraction from the fire was set to 35%, – a typical value representing, for example, wood or kerosene [19].

$$Q(t) = 0.012 \times t^2. \tag{1}$$

Table 1. Models used in the simulations with Alpert's formula, CFX and FDS.

Method	Alpert ceiling jet formula	CFX 4.4	FDS 4.07
Turbulence model	–	RANS k-epsilon	LES
Flow boundary model	Top hat profile	High Reynolds number wall function	Boundary velocity is set to fraction (0.5) of closest node No slip
Grid	–	Symmetry plane Multi-block rectangular grid, stretched	No symmetry plane Rectangular grid
Number of cells		100 mm grid, 47 050 cells 50 mm grid, 73 350 cells	100 mm grid, 2 071 000 cells 50 mm grid, 4 142 000 cells
Wall model	1-D Heat transfer in concrete	Adiabatic $T = 20^{\circ}C$ $T = 40^{\circ}C$	1-D Heat transfer in concrete
Calculation of sprinkler activation	Zone model, Argos with Alpert's formula built-in	Post-processing with Fieldview script	Built-in FDS-model Post-processing with Fieldview script

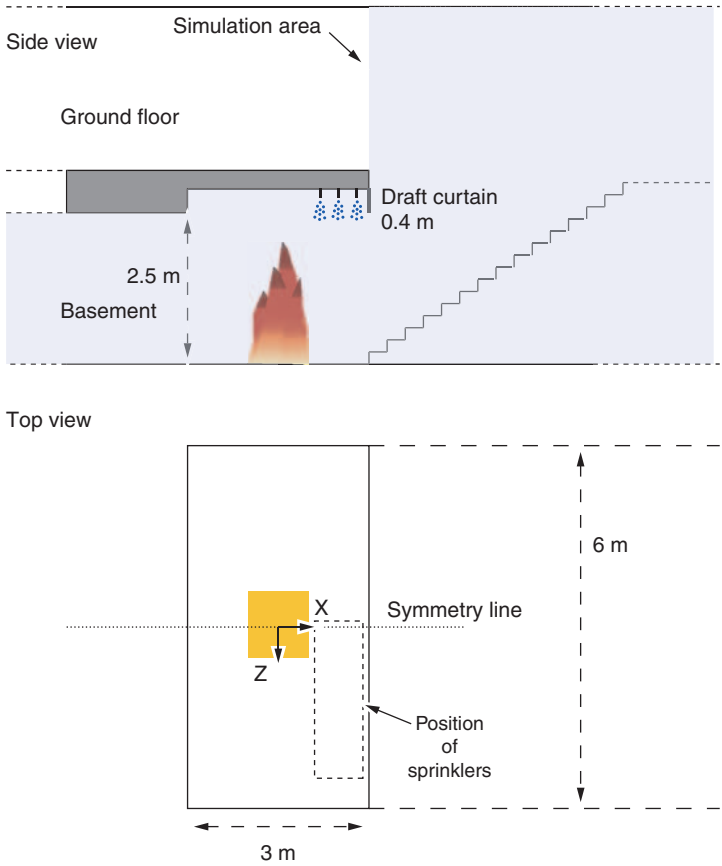

Figure 1. *Geometry of raised ceiling and draft curtain (The color version of this figure is available online).*

In order to check the activation of the sprinklers, the position of the fire was fixed at a $1\,\text{m} \times 1\,\text{m}$ square area on the floor under the center of the raised ceiling area, as in Figure 1. Twelve sprinklers were placed in a grid pattern to give representative values for different positions with coordinates as given in Table 2. The r/H ratio in Table 2 is the radial distance from the center of the fire divided by the ceiling height. These positions were chosen as being between the fire and the draft curtain.

The sprinklers in this example have a glass bulb activated at a temperature of 68°C, and the response time index (RTI) [20] is $38\,(\text{m} \times \text{s})^{1/2}$. Sprinkler skipping caused by cooling of a glass bulb element due to the spray from adjacent active sprinklers has not been included in the simulations; neither has the HRR been affected by the activated sprinklers.

Table 2. Coordinates of sprinklers placed under the raised ceiling.

Sprinkler	Horizontal *x*-coordinate (origin is center of fire) [m]	Horizontal *z*-coordinate (origin is center of fire) [m]	Radial distance *r* from center of fire [m]	*r*/*H* ratio
1	0.7	0.0	0.70	0.24
2	0.7	0.7	0.99	0.34
3	0.7	1.5	1.66	0.57
4	0.7	1.9	2.02	0.70
5	1.0	0.0	1.00	0.34
6	1.0	0.7	1.22	0.42
7	1.0	1.5	1.80	0.62
8	1.0	1.9	2.15	0.74
9	1.3	0.0	1.30	0.45
10	1.3	0.7	1.48	0.51
11	1.3	1.5	1.98	0.68
12	1.3	1.9	2.30	0.79

METHOD FOR CALCULATION OF SPRINKLER ACTIVATION

Ingason [21] showed that the two-parameter model in Equation (2) by Heskestad and Bill [22] is sufficient to mathematically describe the heating of the sprinkler bulb.

$$\begin{aligned} \frac{\mathrm{d}(\mathrm{DT}_{\mathrm{bulb}})}{\mathrm{d}t} &= \frac{\sqrt{U_{\mathrm{jet}}}}{\mathrm{RTI}}\left[\mathrm{DT}_{\mathrm{jet}} - \left(1 + \frac{C}{\sqrt{U}}\right)\mathrm{DT}_{\mathrm{bulb}}\right] \\ \mathrm{DT}_{\mathrm{jet}} &= T_{\mathrm{jet}} - T_{\mathrm{amb}} \\ \mathrm{DT}_{\mathrm{bulb}} &= T_{\mathrm{bulb}} - T_{\mathrm{amb}} \end{aligned} \tag{2}$$

where U_{jet} is the velocity at the ceiling, RTI is the response time index, and C is the heat loss coefficient from the glass bulb sprinkler element to the cold pipe.

For this example, the coefficient C was set to zero and the model thereby reduced to a one-parameter model. One reason for doing this is that the heat detector used to model a sprinkler in FDS does not include the C coefficient. A second reason is that although the two-parameter model delays sprinkler activation, for comparison purposes it is sufficient to use the one-parameter model. The effect of setting the C coefficient to zero was checked using Alpert's formula incorporated in Argos. It showed that using a C coefficient of 0.5, the median value for a quick response sprinkler according to the European sprinkler standard [23], would delay the average sprinkler

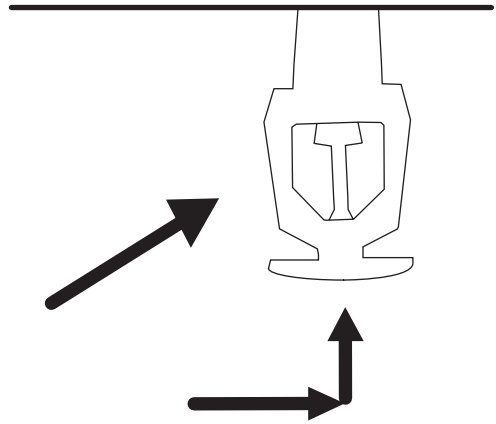

Figure 2. *Deflector plate shields the sprinkler bulb from vertical velocities.*

activation a further 20–25 seconds. As the *C* coefficient is a cooling term, the effect increased with sprinkler activation time and it would therefore increase the difference between the two different setups, but would not change the conclusions.

The flow around the sprinkler head is a complex phenomenon, as described by Ingason [24]. In the cases where separate postprocessor software [25] was used to calculate sprinkler activation, the ceiling jet velocity was set to the horizontal velocity, as the sprinkler deflector plate shields the glass bulb from the vertically rising hot smoke, as in Figure 2. Generally, vertical velocities were very low in the area of interest, so the error introduced by not using this approach is limited.

Considering the differential equation for sprinkler activation, it is evident that the activation time is proportional to the temperature difference between the ceiling jet and the sprinkler glass bulb. It is also proportional to the square root of the velocity. A draft curtain will result in higher temperatures under the ceiling but also tends to slow down smoke close to the draft curtain.

McGrattan et al. [17] showed in a number of large-scale experiments that sprinklers placed close to a draft curtain tend to activate a little sooner compared to sprinklers at the same distance from the fire, but further away from a draft curtain.

Alpert's Ceiling Jet Formula

The response of the sprinkler was also calculated using Equations (3) and (4) from Alpert's ceiling jet correlations [1]. The Alpert ceiling jet

formula assumes that the profile is square (a top hat profile). It does not account for the fact that velocities vary beneath the ceiling. The model is quasi-steady in that it does not include any transport time for the hot gases but assumes that the velocities and temperatures under the ceilings vary synchronously with the HRR. Therefore, the error resulting from using Alpert's formula for an unsteady fire is higher for a fast growing fire compared to a slower growing fire.

If the ratio between r and H is >0.18, it can be assumed that the ceiling jet is horizontal [1]. In the present example, the r/H ratio is >0.18, which means that the sprinklers are outside the impinging region of the fire plume, as shown by the sprinkler coordinates in Table 2, and it is not the fire plume that activates the sprinklers.

The experiments on which the Alpert correlation is based were performed up to an r/H ratio of 1.6 [6]. The r/H ratios for the sprinklers given in Table 2 are all below 1.6 and therefore this requirement is also fulfilled.

$$U_{\text{jet}} = 0.197 \times (Q(t))^{1/3} \times \frac{\sqrt{H}}{r^{5/6}} \quad \text{for } \frac{r}{H} \geq 0.15. \tag{3}$$

$$T_{\text{jet}} = T_{\text{amb}} + \frac{5.38}{H} \times \left(\frac{Q(t)}{r}\right)^{2/3} \quad \text{for } \frac{r}{H} \geq 0.18. \tag{4}$$

A further requirement is that the flame height is less than the ceiling height. The flame height was calculated using Heskestad's formula and a graph of the flame height is shown in Figure 3. The flame height was well below

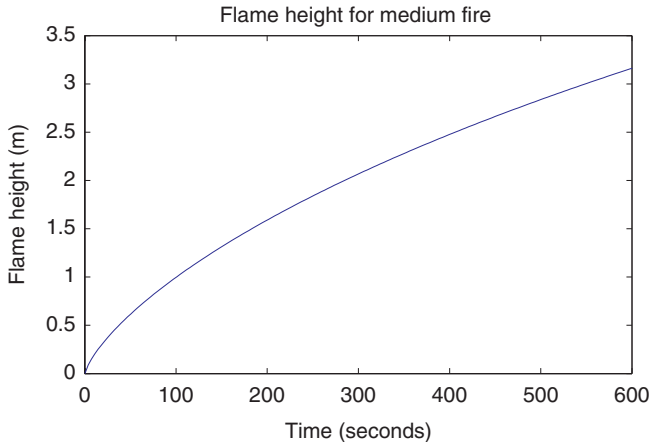

Figure 3. *Flame height calculated using Heskestad's formula (The color version of this figure is available online).*

the ceiling height of 2.9 m up to the time of activation of the sprinklers (around 200 seconds).

The calculations of the activation time are performed using the zone model Argos [3]. In the case with no draft curtain, the geometry is modeled as one big room with a ceiling height of 2.9 m. For the case with the draft curtain, it is modeled as 2 rooms, one room with a ceiling height of 2.9 m and with an opening to the next room with a ceiling height of 2.5 m. In the case with the draft curtain, the higher of either the ceiling jet temperature from Alpert's formula or the smoke layer temperature is used as the temperature around the sprinkler head.

CFX

CFX 4.4 is a RANS model that can handle multi block grids [15]. The simulations in CFX were transient and modeled using the standard k–ε turbulence model with a modified buoyancy term, $C_3 = 1$. The fire was simulated with the eddy break-up model [26] and the fuel was butane.

The geometry was modeled in CFX 4.4 with two different grid sizes, as shown in Table 1. Walls and openings are placed four times the characteristic height of 2.5 and 2.9 m away from the raised ceiling to avoid influencing the results. The overall geometry is thus 25 m long and 30 m wide and there are pressure boundaries at both ends of the dominating flow direction, as shown in Figure 4.

The possibility of using more advanced meshing techniques in CFX (including multi-grid) and the fact that it is a RANS model, makes it possible to reduce the number of cells. Furthermore, a symmetry plane was used at $z = 0$ for the CFX simulations, which reduces the number of cells by half, so that the calculated geometry is 15 m wide (see Figure 5). In the area of the ceiling jet, the cell size in the vertical direction was 100 mm, with 50 mm for the finer grid. The 100 mm grid and the positions of the sprinklers can be seen in Figure 5.

CFX 4.4 lacks a simple transient heat transfer model for a wall, so the walls (including the ceiling) were modeled with three different 'fixed' boundary conditions, adiabatic wall, constant wall temperature of 40°C, and constant wall temperature of 20°C. The ambient temperature was in all simulations 20°C.

In order to adequately resolve the volume where the sprinklers are placed, it is desirable to have a fine grid close to the ceiling. In CFX, a high Reynolds number wall function is used to model the boundary layer. Thus it is a requirement that the cells closest to the wall are outside the regime of a logarithmic profile, which puts a limit on how fine the grid can be. The non-dimensional Y-plus value must preferably be >30 at all times [27].

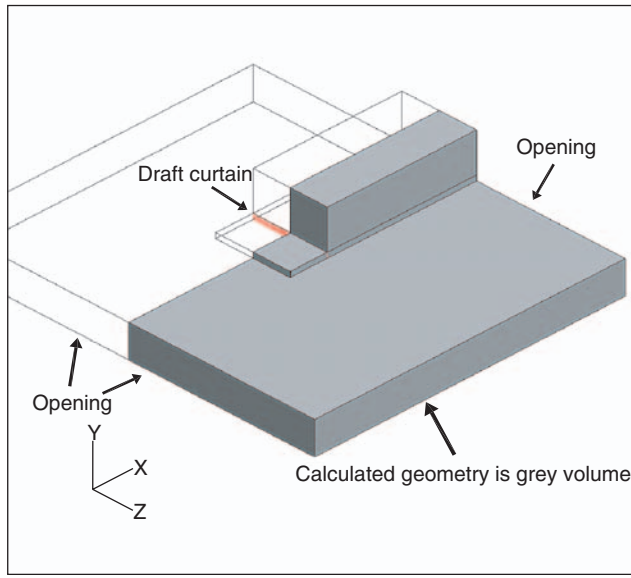

Figure 4. *Modeled geometry in CFX is the gray area (The color version of this figure is available online).*

Figure 6 shows the *Y*-plus values for one of the four CFX geometrical setups with the highest risk of having a low *Y*-plus value due to the draft curtain, as the grid is fine and the velocity is low. It can be seen that the values are larger than 30 in the area of interest. The *Y*-plus requirement was also fulfilled in the other setups at all times, after an initial 5 seconds start-up period.

Calculation of the activation time is performed as a post-processing job for CFX 4.4, as this is a general CFD code without any fire-related features. A script which automatically reads the transient data and calculates the temperature of the sprinkler bulb was developed. The script is written in FVX macro language in Fieldview [25] and it solves the sprinkler Equation (2) using a fully implicit Euler solution.

FDS

In FDS 4.07 the LES model was used [16]. FDS has a built-in transient heat transfer model for walls and the default wall material was set to concrete. The reaction (fuel) was set to methane and the radiation model was used.

A uniform grid with 100 mm grid size in all directions was used for the '100 mm grid'. For the '50 mm grid' the cells were 50 mm only in the

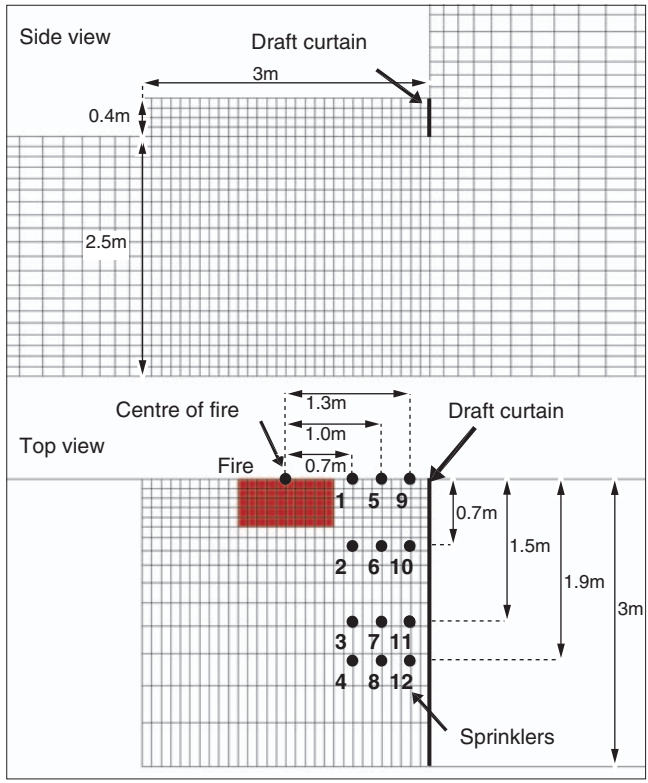

Figure 5. *Area around raised ceiling with sprinkler positions (symmetry plane through the middle for the CFX simulation) (The color version of this figure is available online).*

vertical direction and 100 mm in the other two directions. The number of cells is given in Table 1. The actual grid was modeled as three grids, where the interface between the grids was moved away from the sprinklered area in order to avoid any influence on the results, as shown in Figure 7. Other approaches for modeling the grid in FDS could have been used but this seems to be the safest way to avoid interference at grid interfaces.

The boundary layer in an LES model is an issue of discussion. FDS does not resolve the boundary layer, but instead uses a technique where the velocity at the boundary is set to a fraction of the velocity in the first node [16]. The user can adjust this fraction and two types of calculation have been performed, one calculation with the default fraction of 0.5 and one calculation with zero velocity (no slip) at the boundary.

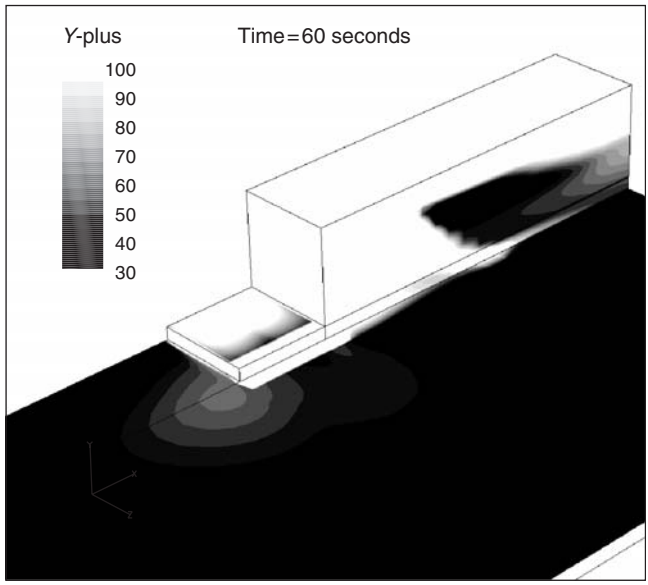

Figure 6. *Y-plus value for a CFX 4.4 simulation with fine grid and draft curtain, $t = 60$ seconds.*

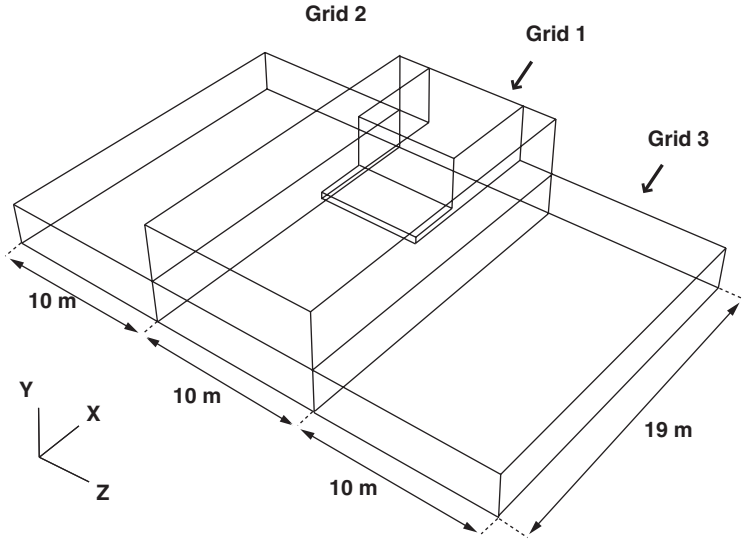

Figure 7. *The geometry in FDS is modeled with three different grids and blocked out cells.*

As FDS is a LES model which resolves the variables in time, the results need to be averaged over a period in order to enable any comparison. For Figures 10 and 11, the results were averaged over a period from 130 to 150 seconds to get an average at 140 seconds.

FDS has a built-in model for calculating heat and sprinkler detector response but the FDS results (velocities and temperatures) were also exported using the Plot3D format and post-processed the same way as the CFX results. The sprinkler activation in FDS was modeled with the use of a heat detector in order to avoid any influence of the sprinkler on the fire. The heat detector calculation in FDS uses Equation (2) with a *C*-value of zero [16].

RESULTS AND DISCUSSION

First, the uncertainties in the calculations will be discussed followed by a comparison of the results of the calculations.

Influence of Heat Transfer to the Ceiling on Activation Time

One uncertainty in the CFX simulations is the wall boundary conditions, as there is no simple transient wall model available. The importance of heat transfer to the ceiling was studied using three different boundary conditions, adiabatic ceiling, ceiling temperature 20°C above the ambient temperature (40°C), and ceiling temperature equal to the ambient temperature (20°C). Adiabatic wall conditions and 20°C at the wall represent the two extremes and 40°C was chosen after performing 1-D heat transfer calculations in Argos.

It can be seen from Table 3 that the ceiling type does not have that great an influence on the activation time of the sprinklers, regardless of the wall being adiabatic or being held on a constant temperature of 40 or 20°C. This is in line with the reported findings of Cooper in Beyler [6]. Furthermore, it can be seen when comparing the ceiling jet profiles for the temperatures at sprinkler positions 10 and 12, that there are only minor differences between the profile for the wall constant at 40°C and the adiabatic wall (see Figures 8 and 9). When comparing different models, the adiabatic wall conditions have been used, as the 50 mm grid was only calculated with the adiabatic wall.

Ceiling Jet Profile for CFX Results

Generally, sprinkler regulations require sprinklers to be placed at a certain distance below the ceiling, in order for them to be in the ceiling jet and thus

Table 3. Activation time of sprinklers in seconds with different boundary conditions in CFX 4.4 for the 100 mm grid and sprinklers located 0.1 m below ceiling.

	Draft curtain			No draft curtain		
Sprinkler number	**Adiabatic Wall [s]**	**Wall 40°C [s]**	**Wall 20°C [s]**	**Adiabatic Wall [s]**	**Wall 40°C [s]**	**Wall 20°C [s]**
1	123	125	126	134	135	136
2	118	122	123	136	139	139
3	124	129	132	142	148	150
4	128	134	137	144	150	154
5	135	139	140	162	164	164
6	121	126	127	144	147	147
7	124	130	132	143	149	151
8	127	133	136	143	150	154
9	136	140	142	183	188	186
10	122	126	128	152	157	157
11	122	127	130	147	153	156
12	124	130	132	145	153	157
Mean	125	130	132	148	153	154
SD	5.4	5.6	5.8	13.2	13.4	12.9

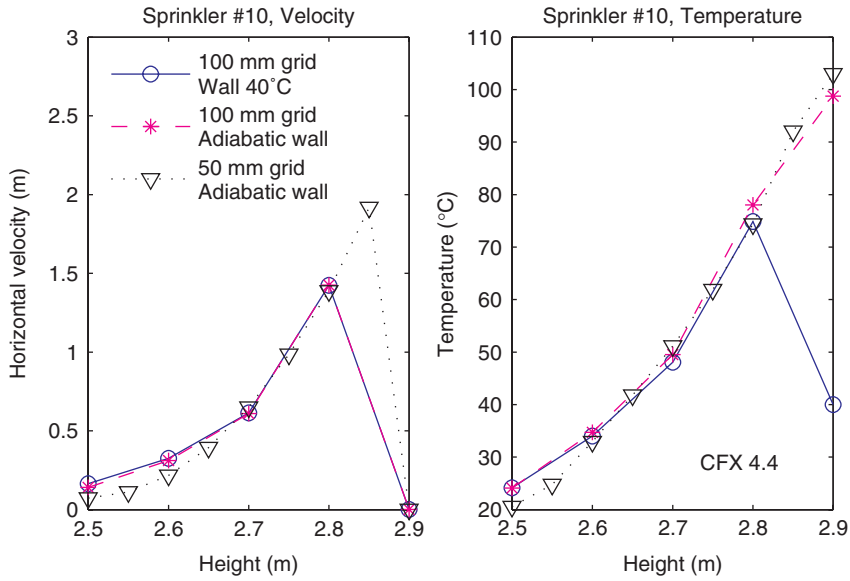

Figure 8. *Velocity and temperature profile in the ceiling jet for three different CFX simulations with no draft curtain at sprinkler position 10 ($r = 1.48$ m), $t = 140$ seconds (The color version of this figure is available online).*

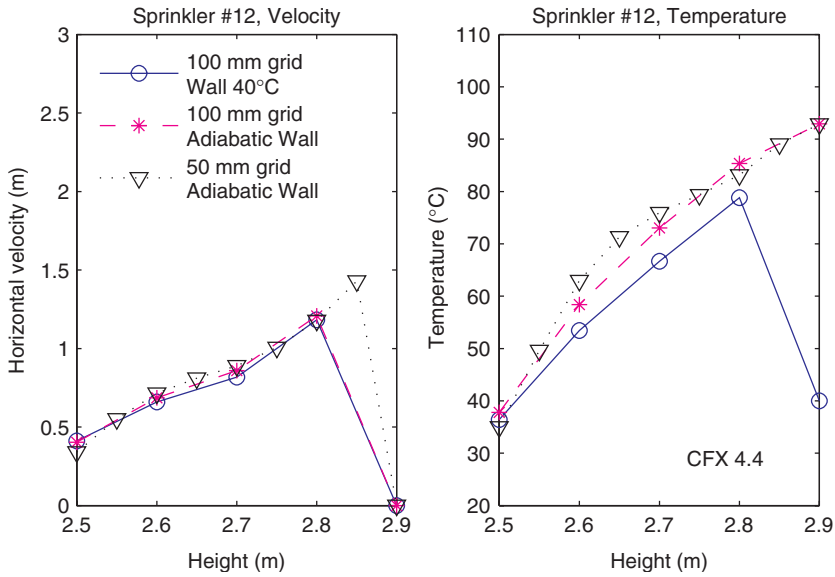

Figure 9. *Velocity and temperature profile in the ceiling jet for three different CFX simulations with no draft curtain at sprinkler position 12 (r = 2.3 m), t = 140 seconds (The color version of this figure is available online).*

obtain a quick response. According to the Danish sprinkler regulations and the European standard for sprinklers, the deflector plate should be placed between 75 and 150 mm below the ceiling [23,28]. For a typical pendant sprinkler, with a distance of 20 mm between bulb and deflector plate, the middle of the sprinkler bulb would then be between 55 and 130 mm below the ceiling. Looking at the ceiling jet profile for the two sprinklers placed closest to the draft curtain (sprinklers 10 and 12), it can be seen that the position of the maximum velocity in the ceiling jet is dependent on the grid size (see Figures 8 and 9). For a grid resolution of 100 mm in the vertical direction, the maximum velocity occurs 100 mm below the ceiling but for the fine grid with 50 mm spacing, the maximum velocity is 50 mm beneath the ceiling. So the exposure of a sprinkler and hence activation time in a simulation is highly dependent on the vertical position of the sprinkler, even if the center of the sprinkler bulb is placed within the limits given by the sprinkler regulations. Furthermore it may be noted that due to the way the data are exported from the calculations, all values are given at cell intersections, whereas the actual velocity is calculated for the middle of the cell.

It may further be noted that the results are not grid independent, when looking at the maximum values. The maximum velocity for sprinkler 10 is 1.5 m/second at 140 seconds for the 100 mm grid, but nearly 2 m/second for

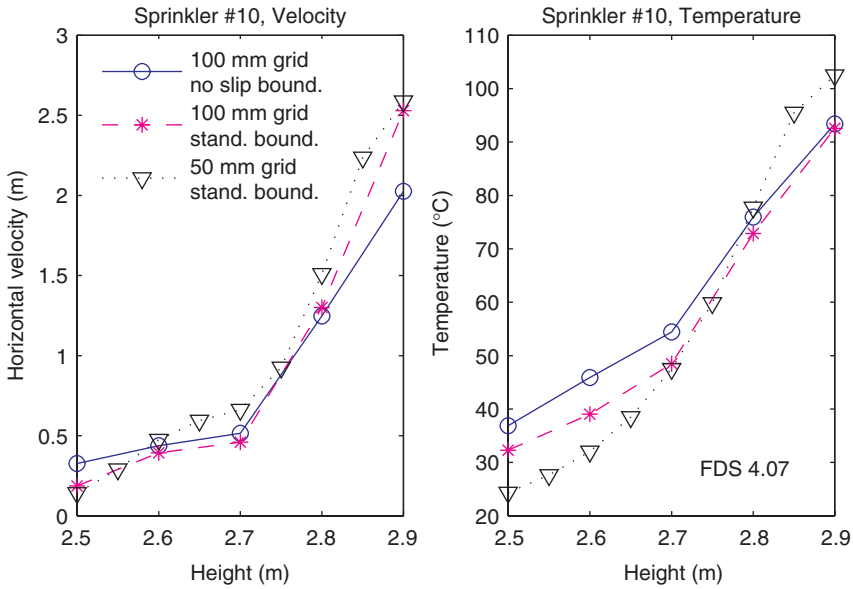

Figure 10. *Velocity and temperature profile in the ceiling jet for three different FDS simulations with no draft curtain at sprinkler position 10 ($r = 1.48$ m), $t = 140$ seconds (The color version of this figure is available online).*

the 50 mm grid, as shown in Figure 8. An even coarser grid with a spacing of 200 mm has also been tried initially and it showed the same tendency.

Ceiling Jet Profile for FDS Results and Influence of Velocity Boundary Conditions

FDS does not resolve the boundary layer; instead it uses a technique where the velocity at the boundary is set to a fraction of the velocity in the first node [16]. The importance of this was studied.

The velocity in the ceiling jet is lower for the no slip boundary compared to the standard boundary conditions without a draft curtain, as in Figures 10 and 11. This is as expected but the lower velocity seems to influence the temperature, because the temperature close to the ceiling is higher for the no slip boundary compared to the standard boundary conditions (see Figures 10 and 11). A possible explanation could be less heat loss to the ceiling, caused by the lower velocity.

It may also be noted that the profiles are grid dependent for the FDS case as well but not with a general tendency biased in one direction as seen for the CFX results, where the finer grid gave higher velocities close to the ceiling.

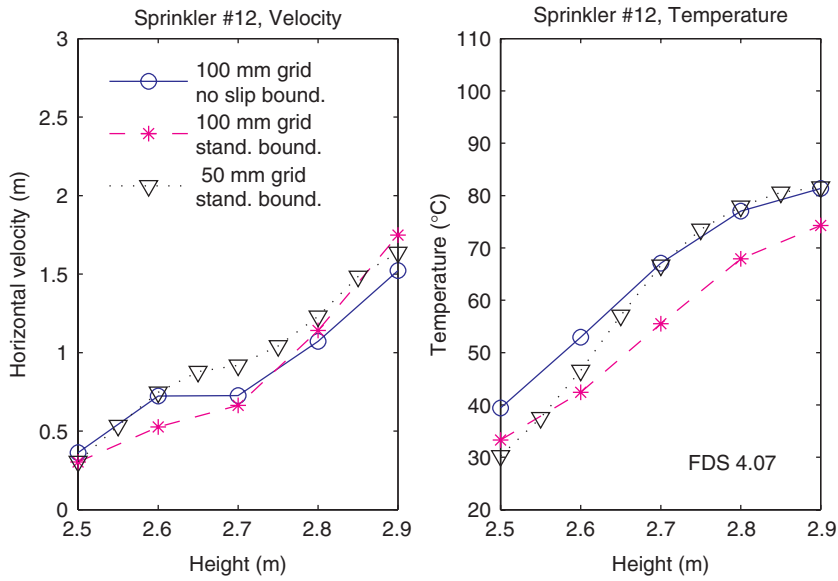

Figure 11. *Velocity and temperature profiles in the ceiling jet for three different FDS simulations with no draft curtain at sprinkler position 12 ($r = 2.3\,m$), $t = 140$ seconds (The color version of this figure is available online).*

Comparing the actual activation times gives only a small difference between the no slip boundary condition and the standard boundary, as seen in Table 4. Sprinklers with standard boundary conditions and therefore higher velocity at the boundary would, as seen previously, be expected to activate first, but actually, the no slip condition gives an earlier sprinkler response. This occurs because of the higher temperature in the no slip case. Presumably, another wall material with less heat capacity and lower conductivity than concrete could interchange these figures. It should also be noted that Zhang et al. [29] found discrepancies in the ceiling region when comparing their FDS results (an earlier release, 2001–2002) with the steady-state experiments of Murakami et al. [13].

In the overall comparison, the standard boundary condition was used, as this gives the longest activation time. Further, the difference is very small and it is the default condition in FDS.

Thickness of Ceiling Jet

To further investigate the properties of the ceiling jet, the thickness of the ceiling jet was compared to the correlation found by Motevalli and Marks [30]. Their basis was a number of small-scale unconfined ceiling jet

Table 4. Activation time of sprinklers using the build-in heat detector in FDS 4.07 with different boundary conditions and 100 mm grid and sprinkler located 0.05 m below ceiling.

	Draft curtain		No draft curtain	
Sprinkler number	**No slip boundary [s]**	**Standard boundary [s]**	**No slip boundary [s]**	**Standard boundary [s]**
1	111	112	112	114
2	118	119	118	122
3	130	134	134	138
4	136	141	140	146
5	120	120	124	130
6	123	125	128	128
7	133	139	144	142
8	139	144	150	154
9	128	129	136	146
10	126	129	136	140
11	133	138	146	150
12	139	142	152	156
Mean	128	131	135	139
SD	8.7	10.4	12.5	13.0

experiments with fires of 0.5–2.0 kW. They developed separate expressions for thermal boundary thickness and momentum thickness. The present calculations do not confirm such differences in thickness and therefore only the expression for the thermal boundary thickness is used (5), as it best fits the numerical results.

$$\frac{L_T}{H} = 0.112 \times \left[1 - \exp\left(-2.24 \times \frac{r}{H}\right)\right] \quad \text{for } 0.26 \leq \frac{r}{H} \leq 2.0 \tag{5}$$

The ceiling jet thicknesses for the CFD simulation were calculated at 140 seconds for the 12 sprinkler positions based on Alpert's $1/e$ depth of the excess temperature profile [31]. For the FDS results, the profile was, as previously, averaged over a period of time. The results are shown in Figure 12. It can be seen that for the sprinklers closest to the center line (sprinklers 1, 2, 5, 6, 9,10), there is a good fit to the correlation by Motevalli and Marks, but for the sprinklers further away (sprinklers 3, 7, 11, 4, 8, 12) and close to the edges at the side, the ceiling jet is thicker. The reason for such a result is the vortex created when the ceiling jet hits the sides of the raised ceiling. The vortex re-circulates the hot ceiling gas back into the ceiling jet, thereby making it thicker. This is an indication of some of the limitations of using

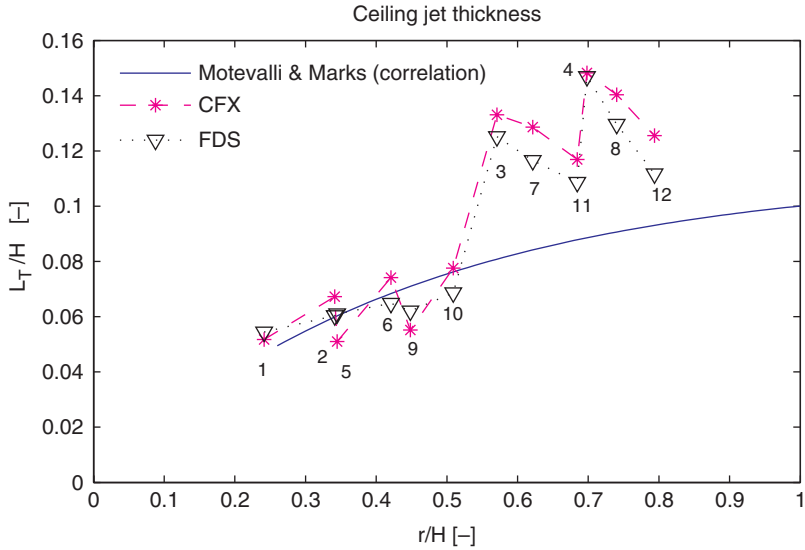

Figure 12. *Comparison of thickness of ceiling jet based on temperature for the 12 different sprinkler positions using correlation of Motevalli and Marks, CFX and FDS, t = 140 seconds (The color version of this figure is available online).*

Alpert's ceiling jet formula, as it will not be able to predict the creation of the vortices.

Vertical Position of Sprinklers for CFX and FDS

As seen previously from the ceiling jet profiles, the vertical position of the sprinkler can have an influence on the activation time, as seen in Figures 8–11. Comparisons of the activation times for the no draft curtain case at different distances below the ceiling show that the CFX results are less sensitive to vertical placement of the sprinklers than the FDS results (see Figure 13). The shortest activation time for the CFX results is with a distance of 0.10 m below the ceiling but the difference to the time for 0.05 m below the ceiling is very small. The shortest activation time for the FDS results is closest to the ceiling – which is in the middle of the first cell for the 100 mm grid. In the previous referred work done by McGrattan et al. [17] the cell size for the simulations were 0.21 m in all three directions and the sprinkler was fixed at 0.08 m below the ceiling, so they did not investigate the influence of the vertical position of the sprinkler.

Furthermore, the results from FDS are the same for distances of 0.10 and 0.15 m below the ceiling when using the routine built into FDS but are

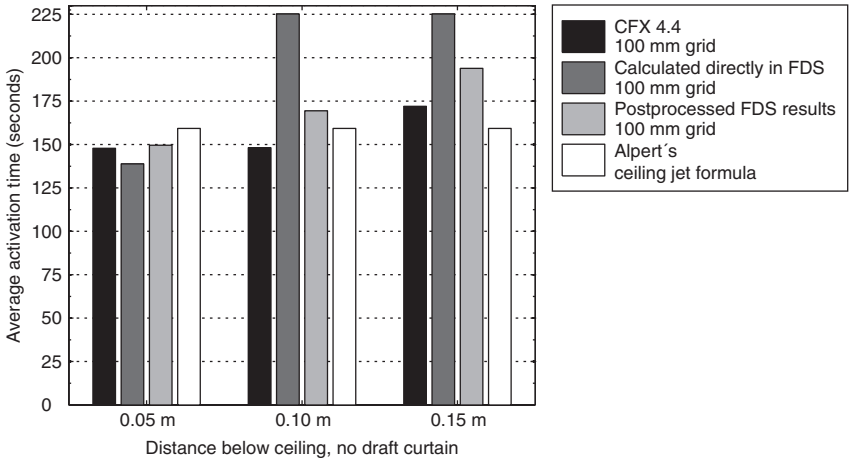

Figure 13. *Average activation time of sprinklers at three different positions calculated with CFX, FDS, and Alpert's ceiling jet formula.*

different when using the routine built into the post-processor [25]. The reason for this is that FDS does not interpolate between the center cell values to arrive at the actual position of the sprinkler heads, but instead uses one value for the entire cell. When exporting the FDS results using the plot3D format to the post processor, the values are interpolated to the cell corners and are therefore smoother. The difference for the two methods in FDS is very small at 0.05 m below the ceiling, which is in the middle of the first cell. Here the center value should be equal to the interpolated value. In the middle of the next cell, at 0.15 m below the ceiling, the same tendency could be expected, but here the differences are larger, – one reason being that sprinkler 9 is first activated after 348 seconds, thereby raising the average activation time.

Comparison with Alpert's formula, which in a way can be used as a reference as it is based on experimental results, shows that the values 0.05 m below the ceiling (center of first cell) are very close to each other. Alpert's ceiling jet formula gives a slightly longer activation time at 0.05 m below the ceiling, but shorter activation time at 0.15 m below the ceiling. At 0.10 m below ceiling, Alpert's formula gives a longer activation time than CFX but a shorter activation time compared with FDS.

Effect of Draft Curtain on Sprinkler Activation Time

Based on the previous observations, since the results seemed to be very dependent on grid size, it was decided for purposes of comparison to

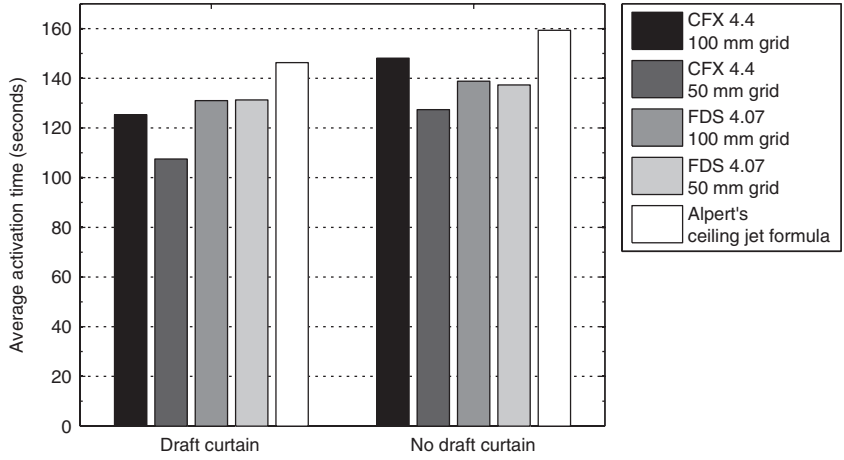

Figure 14. *Average activation time of sprinklers placed in the middle of the first cell in CFX and FDS, and compared to Alpert's ceiling jet formula. Values are taken at middle of first node.*

evaluate sprinkler activation at a location corresponding to the center of the first cell, instead of at a fixed position below the ceiling. Thus for the 100 mm grid, the results were evaluated at 0.05 m below the ceiling and for the 50 mm grid, the results were evaluated at 0.025 m below the ceiling (see Figure 14).

It can be observed that the CFX results are not grid independent. The finer 50 mm grid gives a faster average activation time than the 100 mm grid, for both the case with draft curtain and no draft curtain. The FDS results seem to be more grid independent, though further grid refinement could be needed to fully answer this question. Again, Alpert's ceiling jet formula gives 10–20% slower average sprinkler activation at this position (see Figure 14).

In Table 5, the results for the draft curtain case are compared with the no draft curtain case. The no draft curtain case is used as the basis for comparison. CFX 4.4 shows about 15% reductions in activation times when using a draft curtain for both grids. FDS 4.07 shows about 5% reduction in activation time by using a draft curtain. Finally, Alpert's ceiling jet formula shows about an 8% reduction in activation time when using a draft curtain.

These findings are in line with the experimental results reported by McGrattan et al. [17]. McGrattan et al. performed a series of large-scale sprinkler tests, where the effect of sprinkler activation, smoke ventilation, and draft curtain interaction was studied. An extremely fast growth t^2-fire was used and the ceiling height was 7.6 m for their first test series. It was

Table 5. Reduction in average activation time by using a draft curtain.

	Average reduction in activation time by use of draft curtain
CFX 4.4, 100 mm grid	15%
CFX 4.4, 50 mm grid	16%
FDS 4.07, 100 mm grid	6%
FDS 4.07, 50 mm grid	4%
Alpert's ceiling jet formula	8%

Table 6. Influence of draft curtain on heat release rate (HRR) at average sprinkler activation time.

	Draft Curtain	No draft curtain	
	HRR at average sprinkler activation time [kW]	HRR at average sprinkler activation time [kW]	Reduction of HRR at average sprinkler activation time by use of draft curtain
CFX 4.4, 100 mm grid	189	263	28%
CFX 4.4, 50 mm grid	139	195	29%
FDS 4.07, 100 mm grid	206	231	11%
FDS 4.07, 50 mm grid	207	226	8%
Alpert's ceiling jet formula	257	304	15%

found from these experiments that for two sprinklers, one placed close to the draft curtain, the other placed further away from the draft curtain but both having the same distance from the fire, the one closest to the draft curtain would activate on average 20 seconds before the other sprinkler. The r/H ratio was 0.62, which is similar to the r/H ratio for sprinkler 10 ($r/H = 0.51$) and sprinkler 12 ($r/H = 0.79$) in this study. In percentage, the sprinkler closest to the draft curtain activated on the average 17% faster than the sprinkler further away. The simulations here showed a 5–15% faster response, depending on the method used, so the experimental results qualitatively support the simulation results presented here.

Effect of Draft Curtain on Heat Release Rate at Activation

It is the size of the fire when the sprinkler is activated and not the time to activation, which determines if a sprinkler can control the fire. Table 6 shows the HRR at the average sprinkler activation time. As the fire has a

parabolic growth, the differences with respect to HRR by using a draft curtain are larger, from an 8–29% reduction in HRR.

CONCLUSIONS

The use of draft curtains has some effect on the activation of sprinklers in the scenario under consideration. CFX shows an average reduction in the activation time of 15–16%, whereas FDS only shows an average reduction of 4–6%. The Argos zone model with Alpert's ceiling jet formula gives a reduction of 8% when compared to the no draft curtain case. Looking at the size of the fire at the time of sprinkler activation for the two scenarios, the differences are larger, as the fire used has a parabolic growth. For CFX, FDS, and Alpert's formula, the size of the fire will be respectively 28–29, 8–9, and 16% lower for the draft curtain case than for the no draft curtain case.

Calculation of sprinkler response gave different results in CFX and FDS. The ceiling jet profile moves closer to the ceiling and the maximum values of velocity and temperature increase, when the grid is refined in CFX. Hence in CFX, the activation time is reduced with a finer grid if the sprinkler is positioned in the middle of the first node. The FDS results show little variation in activation time for the two different grid sizes, given the sprinkler is positioned in the middle of the first node. Further calculations are needed to be able to draw conclusions on grid independence for the FDS results.

As could be expected from the ceiling jet profile, the position of the sprinklers in the vertical computational grid has some influence on the activation of the sprinkler in the CFD simulation. FDS is more sensitive than CFX to the vertical position of the sprinklers, one reason being that FDS does not interpolate the center cell values to the actual position of the sprinkler heads. Both CFD programs predict quite well the ceiling jet thickness for the unconfined parts of the ceiling jet, when compared to the correlation provided by Motevalli and Marks.

This study confirmed earlier studies, which showed that heat transfer from the ceiling jet to the ceiling has little influence on the results.

Modeling with CFD can give estimates for the activation time of sprinklers. Using semi-empirical models like Alpert's formula for a position close to the ceiling gives similar results; Alpert's formula gives 10–20% slower average sprinkler activation than the CFD results.

For the specific scenario studied here, Alpert's formula incorporated into a zone model provided results comparable to those from the CFD models, with the added advantage of being much faster and cheaper. However, it

would not have been able to predict recirculation zones, which, in other scenarios, may influence the results.

NOMENCLATURE

$Q(t)$ = heat release rate (HRR) (kW)
t = time (s)
r = radial distance from fire to sprinkler (m)
L_T = ceiling jet thickness
H = ceiling height (m)
T_{jet} = ceiling jet temperature (°C)
T_{amb} = ambient temperature (°C)
T_{bulb} = temperature of sprinkler bulb (°C)
U_{jet} = ceiling jet velocity (m/s)
RTI = response time index $((m \times s)^{1/2})$
C = sprinkler heat loss coefficient $((m \times s)^{1/2})$

ACKNOWLEDGMENTS

Thanks to Brian V. Jensen from DIFT for helping with modeling the case in FDS. The editorial assistance of David Westerman is greatly appreciated.

REFERENCES

1. Alpert, R.L., "Calculation of Response Time of Ceiling-Mounted Fire Detectors," Fire Technology, Vol. 8, 1972, pp. 181–195.
2. Wade, C.A., BRANZFIRE Technical Reference Guide, BRANZ Study Report No 92, Building Research Association of New Zealand, New Zealand, 2004.
3. Husted, B.P. and Soedring, T.W., ARGOS Theory Manual, Danish Institute of Fire Technology, Denmark, 2003.
4. Jones, W.W., Peacock, R.D., Forney, G.P. and Reneke, P.A., CFAST Technical Reference Guide, NIST Special Publication 1026, National Institute of Standards and Technology, Gaithersburg, MD USA, December 2005.
5. Cooper, L.Y., Fire-Plume-Generated Ceiling Jet Characteristics and Convective Heat Transfer to Ceiling and Wall Surfaces in a Two-Layer Zone-Type Fire Environment, NISTIR 4705, National Institute of Standards and Technology, Gaithersburg, MD USA, November 1991.
6. Beyler, C.L., "Fire Plumes and Ceiling Jets," Fire Safety Journal, Vol. 11, No. 1–2, July–September 1986, pp. 53–75.
7. Cooper, L.Y., Report NBSIR 84-2856, National Bureau of Standards, 1984.
8. Nam, S., "Actuation of Sprinklers at High Ceiling Clearance Facilities," Fire Safety Journal, Vol. 39, No. 7, October 2004, pp. 619–642.

9. Motevalli, V., "Numerical Prediction of Ceiling Jet Temperature Profiles during Ceiling Heating Using Empirical Velocity Profiles and Turbulent Continuity and Energy Equations," Fire Safety Journal, Vol. 22, No. 2, 1994, pp. 125–144.
10. Heskestad, G. and Hamada, T., "Ceiling Jets of Strong Fire Plumes," Fire Safety Journal, Vol. 21, No. 1, 1993, pp. 69–82.
11. Hara, T. and Kato, S., "Numerical Simulation of Fire Plume-induced Ceiling Jets Using the Standard k-ε Model," Fire Technology, Vol. 42, 2006, pp. 31–160.
12. Dembsey, N.A., Pagni, P.J. and Williamson, R.B., "Compartment Fire Experiments: Comparison with Models," Fire Safety Journal, Vol. 25, No. 3, October 1995, pp. 187–227.
13. Murakami, S., Kato, S. and Yoshie, R., "Measurement of Turbulence Statistics in a Model Fire Room by LDV," ASHRAE Transactions (Part 2), Vol. 101, Paper No. 3905, 1995, pp. 287–301.
14. Davis, W.D., Forney G.P. and Bukowski, R.W., "Developing Detector Siting Rules from Computational Experiments in Spaces with Complex Geometries," Fire Safety Journal, Vol. 29, No. 2-3, September–October 1997, pp. 129–139.
15. CFX Release 4.4 User Guide, CFX International, AEA Technology, Harwell Laboratory, Oxfordshire, UK 2001.
16. McGrattan, K. and Forney, G., Fire Dynamics Simulator (Version 4) User's Guide, NIST Special Publication 1019, National Institute of Standards and Technology, Gaithersburg, MD USA, March 2006.
17. McGrattan, K.B., Hamins, A. and Stroup, D.W., Sprinkler, Smoke and Heat Vent, Draft Curtain Interaction - Large Scale Experiments and Model Development, Technical Report NISTIR 6196-1, 158 pages, National Institute of Standards and Technology, Gaithersburg, MD USA, September 1998.
18. NFPA 204, Standard for Smoke and Heat Venting, National Fire Protection Association, Quincy, MA USA, 2002 Edition.
19. Tewarson, A., "Generation of Heat and Chemical Compounds in Fires," In: DiNenno, P. (ed.), SFPE Handbook of Fire Protection Engineering, 3rd edn, National Fire Protection Association, Quincy, MA USA, 2002.
20. Heskestad, G. and Smith, H.F., Investigation of a New Sprinkler Sensitivity Approval Test; The Plunge Test, FMRC 22485, Factory, Mutual Research Corporation, Norwood, MA USA, December 1976.
21. Ingason, H., "Investigation of Thermal Response of Glass Bulb Sprinklers using Plunge and Ramp Tests," Fire Safety Journal, Vol. 30, No. 1, February 1998, pp. 71–93.
22. Heskestad, G. and Bill, R.G., "Quantification of Thermal Responsiveness of Automatic Sprinklers Including Conduction Effects," Fire Safety Journal, Vol. 14, 1988, pp. 113–125.
23. EN 12845:2004, Fixed Fire Fighting Systems, Automatic Sprinkler Systems, Design, Installation and Maintenance, CEN, European Committee for Standardization, Brussels, September 2004.
24. Ingason, H., Investigation of Sprinkler Response Models and the Interaction between Sprinklers and Fire Vent, Rapport 1008, Brandteknik, Lund University, Sweden 1992.
25. Fieldview Reference Manual, Software release 11, Intelligent Light, Rutherford, NJ 07070 USA, 2005.
26. Magnussen, B.F. and Hjertager, B.H., "On the Mathematical Modelling of Turbulent Combustion with Special Emphasis on Soot Formation and Combustion," Sixteenth Symposium (International) on Combustion, The Combustion Institute, Pittsburgh, 1976, pp. 1405–1414.
27. Versteeg, H. and Malalasekera, W., An Introduction to Computational Fluid Dynamics: The Finite Volume Method Approach, Longman, Great Britain, 1995.
28. Automatiske sprinkleranlaeg (in Danish), Forskrift 251, Danish Institute of Fire and Security Technology, Denmark, January 2001.

29. Zhang, W., Hamer, A, Klassen, M., Carpenter, D. and Roby, R., "Turbulence Statistics in a Fire Room Model by Large Eddy Simulation," Fire Safety Journal, Vol. 37, No. 8, November 2002, pp. 721–752.
30. Motevalli, V. and Marks, C.H., "Characterizing the Unconfined Ceiling Jet under Steady-state Conditions; A Reassessment," Fire Safety Science, Proc. 3rd International Symposium, Elsevier, New York, USA, 1991, pp. 301–12.
31. Alpert, R., "Ceiling Jet Flows," In: DiNenno, P. (ed.) SFPE Handbook of Fire Protection Engineering, 3rd edn, National Fire Protection Association, Quincy, MA USA, 2002.